Control of Graphene Field-Effect Transistors by Interfacial Hydrophobic Self-Assembled Monolayers

Wi Hyoung Lee, Jaesung Park, Youngsoo Kim, Kwang S. Kim, Byung Hee Hong,* and Kilwon Cho**

Graphene has received considerable attention as a potential alternative material for use in next-generation semiconductor technology.[1,2] Since its discovery, graphene-based electronic devices have been fabricated on SiO_2/Si substrates to take advantage of the optical contrast between the monolayer graphene and SiO_2 and because of the ease of fabrication of devices with metal-oxide-semiconductor (MOS) structures.[3] The performances of graphene field-effect transistors (FETs) on SiO_2 substrates, however, are limited by charged impurity scattering,[4,5] extrinsic scattering by surface phonons,[6] resonant scattering from atomic scale defects,[7] and corrugation or doping by residual adsorbates.[8,9]

To overcome these performance limits, a buffer layer may be inserted between graphene and the gate dielectric to modify the surface properties of SiO_2. This approach provides an alternative method for reducing charged impurity scattering or adsorbate-limited doping. For example, hexamethyldisilazane (HMDS),[10] phenyl-terminated organosilane,[11] or polymeric buffer layers[12] have been used to reduce the intrinsic doping levels, thereby enhancing the electrical properties of graphene FETs. However, the mechanism by which the electrical properties of graphene FETs are affected has not been elucidated and systematic studies of the effects of buffer layers on the performance of graphene FETs are needed. Previous experiments have mainly tested mechanically exfoliated graphene flakes. Because the exfoliation process depends on the surface properties of the substrate, large variations between samples are expected from this source of graphene. To this end, recent chemical vapor deposition (CVD) methods have enabled the synthesis of large-area uniform high-quality graphene. The benefits of CVD graphene were employed in the systematic study of buffer layers in graphene FETs reported here.[13,14]

A systematic study of the effects of a buffer layer on the performance of graphene FETs was conducted using CVD-grown large-area graphene. The chemical and physical properties of graphene/dielectric (SiO_2) interfaces were controlled by treating SiO_2 substrates with hydrophobic self-assembled monolayers (SAMs) of two organoalkyl silanes, octyltrichlorosilane (OTS) and octadecyltrichlorosilane (ODTS), with varying alkyl chain lengths (C8 and C18, respectively) as well as the previously described HMDS with an alkyl chain length of C1. These buffer layers modified the chemical and physical nature of the interface with graphene, which modulated the electrical response of the graphene FETs. Thus, the performances of graphene FETs were significantly improved by the presence of a SAM buffer layer.

SAMs may be fabricated in a simple and straightforward manner. OTS and ODTS-SAMs spontaneously self-assembled on gate-dielectric (SiO_2) surfaces via a surface reaction involving hydrolysis and condensation (see the Experimental Section for details).[15] The HMDS buffer layer was prepared on the SiO_2 surface by spin-coating.[16] The physical characteristics of the SAMs and the surface wettability of the SAM-modified SiO_2 surfaces are listed in **Table 1**. As expected, the thickness of the SAMs increased with increasing alkyl chain length. The chain packing density of the SAMs was evaluated by X-ray photoemission spectroscopy (XPS), as shown in **Figure 1**a,b. The intensity of a single C_{1s} peak at 284.6 eV increased with increasing alkyl chain length (HMDS < OTS < ODTS). In parallel, the Si_{2p} peaks at 99.3 (Si^0) and 103.3 (Si^{4+}) eV decreased with increasing alkyl chain length (HMDS > OTS > ODTS) due to the increasing thickness of the SAMs prepared on the SiO_2/Si substrate. The C_{1s}/Si_{2p} peak ratio, normalized by thickness of SAMs, was used as a measure of the relative chain packing density.[17–19] ODTS-SAMs exhibited a high packing density (10%) relative to the packing densities of HMDS and OTS-SAMs. This observation was investigated by characterizing the physical structures of OTS- and ODTS-SAMs by Fourier transform infrared (FTIR) spectroscopy. As the number of C atoms increased from 8 (OTS) to 18 (ODTS), the positions of the peaks corresponding to the symmetric and asymmetric CH_2 vibrations shifted to lower wavenumbers, from 2855 to 2851 cm^{-1} and from 2927 to 2920 cm^{-1}. These shifts indicated that the ordering of the alkyl chains in the SAMs changed from disordered (OTS) to ordered (ODTS). Trans alkyl chain conformations were favored by van der Waals forces between longer alkyl chains.[18,20] The increased prevalence in trans alkyl chain conformations in turn increased the packing density in ODTS-SAMs. On the

Dr. W. H. Lee, Prof. K. Cho
Department of Chemical Engineering
Pohang University of Science and Technology
Pohang, 790-784, Republic of Korea
E-mail: kwcho@postech.ac.kr
J. Park, Prof. K. S. Kim
Center for Superfunctional Materials
Department of Chemistry
Pohang University of Science and Technology
Pohang, 790-784, Republic of Korea
E-mail: kim@postech.ac.kr
Y. Kim, Prof. B. H. Hong
Department of Chemistry
Sungkyunkwan University
Suwon, 440-746, Republic of Korea
E-mail: byunghee@skku.edu

DOI: 10.1002/adma.201101340

Table 1. Characteristics of various SAM-modified SiO_2/Si substrates.

	Thickness [Å]	C_{1s}/Si_{2p} ratio	Surface energy [mJ/m^2]	RMS roughness [Å]
HMDS	3	0.67	45	3
OTS	8	0.66	28	4
ODTS	22	0.73	26	4

other hand, the HMDS-modified SiO_2 surface did not display CH_2 vibrations from the single alkyl chain (Figure 1d). HMDS only reacted with the silanol groups in SiO_2 and did not engage in a self-condensation process (Si-O-Si bonds). Owing to the limited reaction sites on the single-chain HMDS, the surface energy of the HMDS-modified SiO_2 was much higher than the surface energies of OTS- and ODTS-SAMs-modified SiO_2 (see Table 1).[16]

CVD-grown monolayer graphene was transferred from a copper foil to a SiO_2/Si substrate to evaluate the chemical and physical interactions between the graphene and various SAM-modified SiO_2 substrates (see the Experimental Section). The chemical and physical properties of graphene on various SAM-modified SiO_2 substrates were investigated using Raman spectroscopy, as shown in **Figure 2**a. The 2D band intensity increased with increasing alkyl chain length (untreated < HMDS < OTS < ODTS). Furthermore, the positions of the G bands on the OTS and ODTS SAM-modified SiO_2 substrates were clearly red-shifted relative to the peak positions of the untreated SiO_2 substrate. The intensity ratio between the 2D band and the G band, as well as the full width at half maximum (FWHM) of the 2D band, was sensitive to the doping levels in a graphene sample.[21] Whereas the 2D-band/G-band intensity ratio systematically increased with increasing alkyl chain length, the width of the 2D width showed the opposite trend. The changes in peak intensity and width clearly demonstrated that doping was effectively reduced using a SAM buffer layer with long alkyl chains.

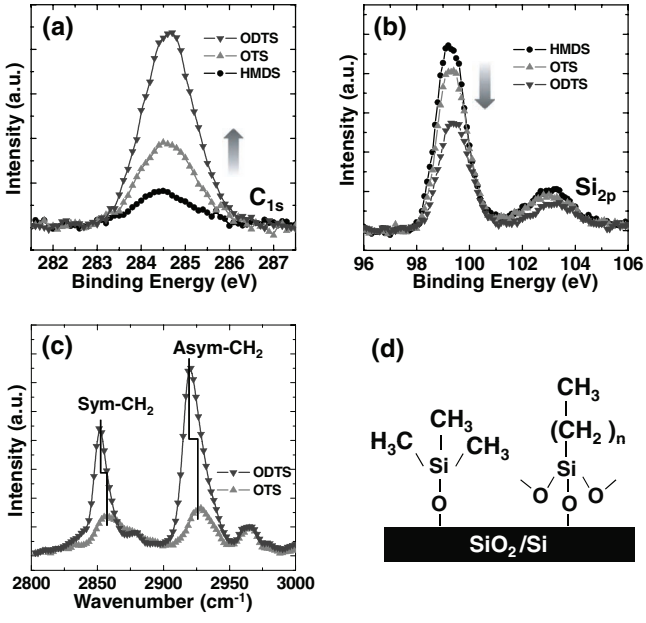

Figure 1. XPS spectra representing a) C_{1s} and b) S_{2p} binding energy peaks of various SAMs-modified SiO_2/Si substrates. c) FTIR spectra of the methylene (CH_2-) vibration of various SAMs with different alkyl chain length (C) (OTS: C8, ODTS: C18). d) Chemical structures of the HMDS-modified (left) and organosilane-modified (right) SiO_2/Si substrates (OTS for n = 7 and ODTS for n = 17).

The doping characteristics were further characterized by calculating the work functions of the graphene films from the ultraviolet photoemission spectra, as shown in Figure 2c. The change in the onset of the secondary electrons corresponded to the change in the work function in graphene according to

$$\phi = \hbar\omega - |E_{sec} - E_{FE}| \quad (1)$$

where $\hbar\omega$ = 21.2 eV (He I source), E_{sec} is the onset of the secondary emission, and E_{FE} is the Fermi edge (22.0 eV from the valence band spectrum, under a sample bias of –5 V, measured at the 4B1 beamline at Pohang Accelerator Laboratory). The work function of graphene decreased with increasing SAM alkyl chain length, giving work functions of 4.5 eV for the untreated SiO_2 and 4.25 eV for ODTS-modified SiO_2 (Figure 2d). Graphene on SiO_2/Si substrates displays hole doping characteristics due to charge transfer from the graphene to various adsorbates, such as O_2 and water molecules, on the SiO_2 surface.[10,22] When SAMs are constructed on a SiO_2 surface, the buffer layers can effectively block most reactive sites (i.e., silanol groups) in SiO_2 to prevent the coupling of adsorbates to SiO_2. The blocking efficiency differs according to the bonding characteristics, physical structure, and chain packing density of the SAM. Ordered and closely packed ODTS SAMs exhibited the highest blocking efficiencies to suppress hole doping. Thus, graphene on ODTS SAMs exhibited the lowest work function. On the other hand, HMDS blocked the SiO_2 surface weakly due to limitations in the self-condensation process in the presence of a single alkyl chain. Thus, the magnitudes of hole doping obtained from the graphene work functions were ordered as follows: ODTS < OTS < HMDS < untreated.

The effects of the SAM buffer layer on the electrical properties of the graphene films were examined by depositing Au source/drain electrodes directly onto the graphene films without the use of photolithography processes (**Figure 3**a). Figure 3b shows the conductivities of graphene FETs on various SAMs-modified SiO_2/Si substrates as a function of the gate voltage V_G. The Dirac point voltage V_G^{Dirac}, the point at which the majority of the carrier population shifts from one type to another, gradually changed from 52 V for untreated SiO_2 to 24 V for ODTS-modified SiO_2 substrates. Because this transition voltage was determined by the excess charge carriers remaining on the graphene, it was directly correlated with the doping type and magnitude in the graphene films.[23] As shown in Figure 3c, V_G^{Dirac} shifted further from V_G = 0 V as the alkyl chain length of the SAMs increased (i.e., as the blocking efficiency of the SAMs was enhanced). These results indicate that hole doping was effectively screened by SAMs with long alkyl chains, as demonstrated in Figure 2. The positive value of V_G^{Dirac}, even for graphene FETs supported on ODTS-modified SiO_2, may be attributed to the unintentional doping of graphene, for

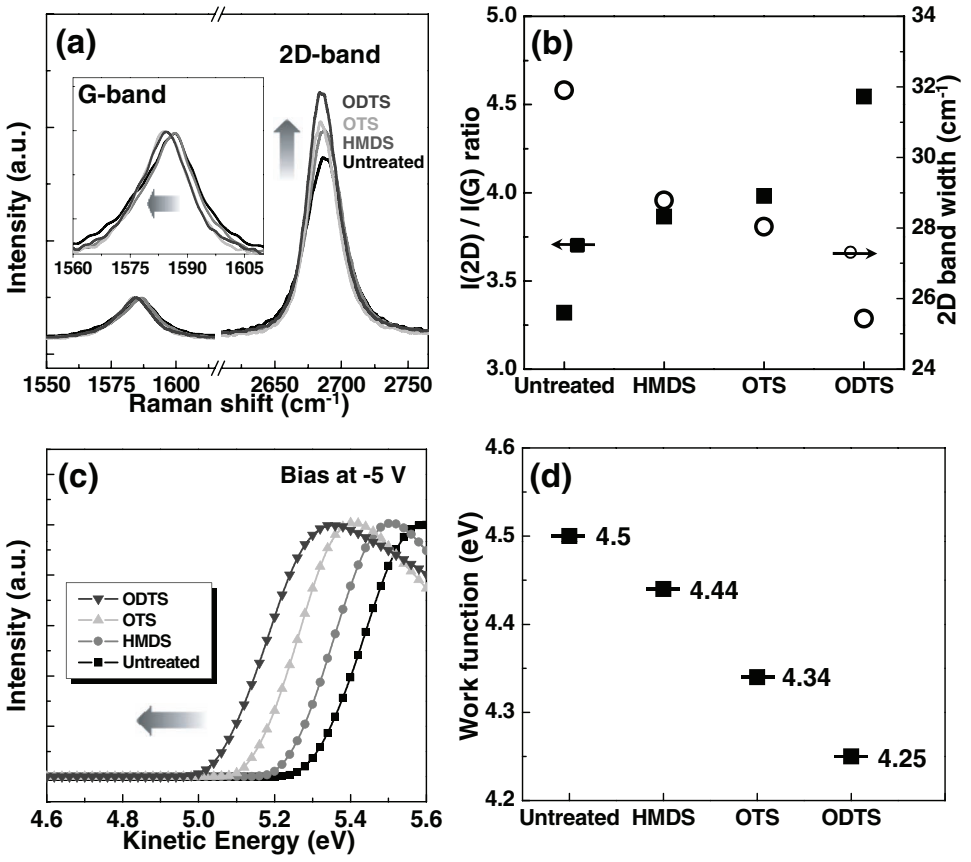

Figure 2. a) Raman spectra of monolayer graphene on various SAMs-modified SiO_2/Si substrates. The inset shows magnified spectra of G bands. b) Comparative plots of the I(2D)/I(G) ratios and 2D-band widths. c) Ultraviolet photoemission spectra (at the secondary electron emission region) of monolayer graphene on various SAM-modified SiO_2/Si substrates. d) A comparative plot of the graphene work functions.

example by poly(methyl methacrylate) (PMMA) residues on the graphene surface.[8]

The carrier mobility was calculated in the linear regime using[2]

$$\mu = \frac{1}{C_i}\frac{d\sigma}{dV_G} = \frac{Lg_m}{WC_iV_D} \quad (2)$$

where $C_i = 1.08 \times 10^{-8}$ F cm^{-2}, $g_m = dI_D/dV_G$, $V_D = 0.01$ V, $L = 30$ μm, and $W = 300$ μm.

The electron and hole mobilities calculated in the linear regime increased with increasing SAM alkyl chain length according to: untreated < HMDS < OTS < ODTS (Figure 3d). The observed asymmetry in hole and electron mobilities may be due to scattering cross section differences for the holes and electrons[24] or drift in the charged impurities from the substrate.[25] Noticeably, both the electron and hole mobilities increased more than three-fold for buffer layers made from SAMs with long alkyl chains. Because the surface roughness observed after deposition of the SAMs on the SiO_2 did not decrease (Table 1), the enhanced mobility was directly correlated with the effective screening of the SiO_2 surface, which has previously been reported to limit the graphene mobility due to charged impurities.[4,5,25] The mobilities obtained in our experiments were relatively low and corresponded to the diffusive transport regime. Charged impurity scattering may provide the prevailing scattering mechanism if residual impurities in graphene are responsible for carrier transport under electron and hole puddles.[4,25] The carrier density n in graphene induced by V_G in the presence of impurity doping was calculated using[26]

$$n = \eta\left(V_G - V_G^{Dirac}\right) \quad (3)$$

where $\eta = 7.2 \times 10^{10}$ cm^{-2} V^{-1}. Figure 3e shows a plot of the conductivity as a function of the carrier density near V_G^{Dirac}. The minimum conductivity (i.e., $\sigma(V_G = V_G^{Dirac})$) and the plateau width at the minimum conductivity depended on the identity of the SAMs inserted between the graphene and the SiO_2 surface. We emphasize that the trends in 1) V_G^{Dirac}, 2) electron and hole mobilities, 3) the minimum conductivity, and 4) the plateau width agreed well with the carrier transport mechanism for charged impurity scattering.[25] As the density of charged impurities decreased, the FETs exhibited lower V_G^{Dirac} values, higher hole/electron mobilities, higher minimum conductivities, and narrower plateau widths. Furthermore, the sublinear conductivity at high V_G, which was clearly observable in the transconductance (g_m) curve for the ODTS SAM, as shown in Figure 3f, was correlated with the change in the scattering mechanism from long-range scattering to short-range scattering.[4,25] The electrical measurements confirmed that the

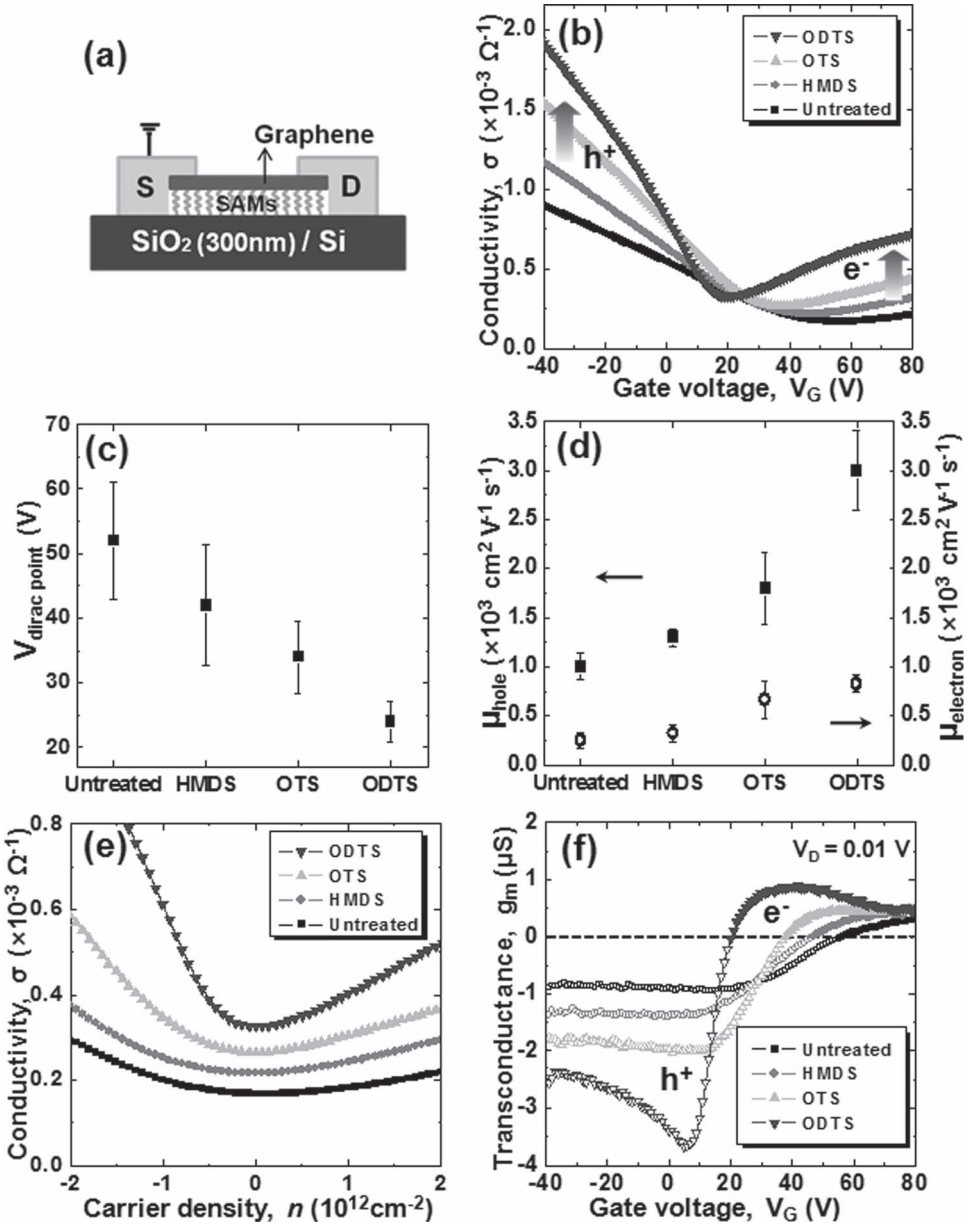

Figure 3. a) Schematic diagram showing the graphene FETs having SAMs as buffer layers between graphene and the SiO_2 substrate. b) The conductivity of the graphene FETs formed from SAM-modified SiO_2/Si substrates as a function of gate voltage (V_G). c) Comparative plot of the Dirac-point voltages. d) Comparative plots of electron and hole field-effect mobilities. e) Detailed view of the density-dependent conductivity near the Dirac point for the graph in (b). f) Transconductance g_m of the graphene FETs on various SAM-modified SiO_2/Si substrates as a function of V_G.

SAMs with long alkyl chain lengths effectively screened charged impurities originating from the adsorbates on the SiO_2 surface, and thus reduced the graphene doping and enhanced the electrical properties of the graphene FETs when inserted between graphene and SiO_2.

In conclusion, we report systematic studies of the effects of various hydrophobic SAMs inserted between CVD-grown large-area graphene and SiO_2 substrates. As the SAM alkyl chain length increased, substrate-induced doping of the graphene decreased, and thus the graphene FETs exhibited higher hole/electron mobilities with lower Dirac point voltages. Furthermore, changes in the electrical performances in the presence of SAMs could be explained by charged impurity scattering, indicating that charged impurities in graphene could be tuned by the alkyl chain length of a SAM inserted between the graphene and the SiO_2 substrate. Our study demonstrated that charged impurity scattering arises from the chemical and physical properties of the substrate surface as well as from the intrinsic quality of graphene. Thus, appropriate surface chemistries at graphene/dielectric interfaces are essential for enhancing the electrical properties of graphene FETs.

Experimental Section

Materials and device fabrication: OTS and ODTS-SAMs were fabricated on SiO_2/Si substrates following the procedure reported in the literature.[19] HMDS was spin-coated onto a clean SiO_2/Si substrate, and the substrate was baked at 150 °C for 1 h. Graphene was synthesized following the CVD process reported in the literature.[14,27] As-grown monolayer graphene films on a copper foil were covered with PMMA (M_w = 240 kg mol^{-1}) and floated in an aqueous solution of 0.1 M ammonium persulfate ($(NH_4)_2S_2O_8$) solution. After all copper layers had been etched away, the graphene film with the PMMA support was transferred to various SAM-modified SiO_2 (300 nm, capacitance 10.8 nF cm^{-2})/Si substrates. The graphene film remained on the silicon substrate after the PMMA support had been removed with acetone. To define source/drain electrodes in graphene FETs, Au was thermally evaporated through a shadow mask (channel length: 30 μm, channel width: 300 μm).

Characterization: The surface energies of the prepared SAMs were determined by measuring the contact angles of two probe liquids (deionized water and diiodomethane).[28] The thickness of the SAMs was determined using an ellipsometer (M-2000V, J. A. Woollam), and the root-mean-square (rms) roughness was examined by atomic force microscopy (AFM, Digital Instruments). The relative chain packing density of the SAMs was characterized by X-ray photoelectron spectroscopy using a VG ESCALAB 220i spectrometer with an Al Kα X-ray line (1486.6 eV). Chain conformation was investigated by FTIR spectroscopy (Bruker IFS 66v). The optical properties of graphene films were obtained by Raman spectroscopy (Renishaw, RM-1000 Invia) with an excitation energy of 2.41 eV (514 nm, Ar^+ ion laser). The work functions of graphene films were characterized by measuring the secondary electron cutoff spectra by ultraviolet photoelectron spectroscopy (UPS; He I source, $h\nu$ = 21.2 eV) at the 4B1 beamline of the Pohang Accelerator Laboratory in Korea. The current–voltage characteristics of the graphene FETs were analyzed using Keithley 2636A semiconductor parameter analyzers.

Acknowledgements

W. H. Lee and J. Park contributed equally to this work. This research was supported by National Research Foundation (NRF) grant (No. 2009-0093485), NRF (National Honor Scientist Program, 2010-0020414), Converging Research Center Program (2010K001066), and Basic Science Research Program (2011-0006270) through the National Research Foundation of Korea (NRF). The authors thank the Pohang Accelerator Laboratory for providing the synchrotron radiation sources at 4B1 and 8A2 beam lines used in this study.

Received: April 9, 2011
Published online: July 4, 2011

[1] a) A. K. Geim, *Science* **2009**, *324*, 1530; b) Y. W. Zhu, S. Murali, W. W. Cai, X. S. Li, J. W. Suk, J. R. Potts, R. S. Ruoff, *Adv. Mater.* **2010**, *22*, 3906; c) M. J. Allen, V. C. Tung, R. B. Kaner, *Chem. Rev.* **2010**, *110*, 132; d) K. P. Loh, Q. L. Bao, P. K. Ang, J. X. Yang, *J. Mater. Chem.* **2010**, *20*, 2277.
[2] F. Schwierz, *Nat. Nanotechnol.* **2010**, *5*, 487.
[3] a) K. S. Novoselov, A. K. Geim, S. V. Morozov, D. Jiang, Y. Zhang, S. V. Dubonos, I. V. Grigorieva, A. A. Firsov, *Science* **2004**, *306*, 666; b) K. S. Novoselov, A. K. Geim, S. V. Morozov, D. Jiang, M. I. Katsnelson, I. V. Grigorieva, S. V. Dubonos, A. A. Firsov, *Nature* **2005**, *438*, 197; c) Y. B. Zhang, Y. W. Tan, H. L. Stormer, P. Kim, *Nature* **2005**, *438*, 201.
[4] S. Adam, E. H. Hwang, V. M. Galitski, S. Das Sarma, *Proc. Natl. Acad. Sci. USA* **2007**, *104*, 18392.
[5] J. H. Chen, C. Jang, S. Adam, M. S. Fuhrer, E. D. Williams, M. Ishigami, *Nat. Phys.* **2008**, *4*, 377.
[6] J. H. Chen, C. Jang, S. D. Xiao, M. Ishigami, M. S. Fuhrer, *Nat. Nanotechnol.* **2008**, *3*, 206.
[7] Z. H. Ni, L. A. Ponomarenko, R. R. Nair, R. Yang, S. Anissimova, I. V. Grigorieva, F. Schedin, P. Blake, Z. X. Shen, E. H. Hill, K. S. Novoselov, A. K. Geim, *Nano Lett.* **2010**, *10*, 3868.
[8] M. Ishigami, J. H. Chen, W. G. Cullen, M. S. Fuhrer, E. D. Williams, *Nano Lett.* **2007**, *7*, 1643.
[9] D. B. Farmer, R. Golizadeh-Mojarad, V. Perebeinos, Y. M. Lin, G. S. Tulevski, J. C. Tsang, P. Avouris, *Nano Lett.* **2009**, *9*, 388.
[10] M. Lafkioti, B. Krauss, T. Lohmann, U. Zschieschang, H. Klauk, K. von Klitzing, J. H. Smet, *Nano Lett.* **2010**, *10*, 1149.
[11] Y. M. Shi, X. C. Dong, P. Chen, J. L. Wang, L. J. Li, *Phys. Rev. B* **2009**, *79*, 115402.
[12] S. S. Sabri, P. L. Levesque, C. M. Aguirre, J. Guillemette, R. Martel, T. Szkopek, *Appl. Phys. Lett.* **2009**, *95*, 242104.
[13] K. S. Kim, Y. Zhao, H. Jang, S. Y. Lee, J. M. Kim, K. S. Kim, J. H. Ahn, P. Kim, J. Y. Choi, B. H. Hong, *Nature* **2009**, *457*, 706.
[14] X. S. Li, W. W. Cai, J. H. An, S. Kim, J. Nah, D. X. Yang, R. Piner, A. Velamakanni, I. Jung, E. Tutuc, S. K. Banerjee, L. Colombo, R. S. Ruoff, *Science* **2009**, *324*, 1312.
[15] a) A. Ulman, *Chem. Rev.* **1996**, *96*, 1533; b) S. A. DiBenedetto, A. Facchetti, M. A. Ratner, T. J. Marks, *Adv. Mater.* **2009**, *21*, 1407; c) W. H. Lee, J. H. Cho, K. Cho, *J. Mater. Chem.* **2010**, *20*, 2549.
[16] J. A. Lim, W. H. Lee, D. Kwak, K. Cho, *Langmuir* **2009**, *25*, 5404.
[17] Y. L. Wang, M. Lieberman, *Langmuir* **2003**, *19*, 1159.
[18] H. S. Lee, D. H. Kim, J. H. Cho, M. Hwang, Y. Jang, K. Cho, *J. Am. Chem. Soc.* **2008**, *130*, 10556.
[19] D. H. Kim, H. S. Lee, H. C. Yang, L. Yang, K. Cho, *Adv. Funct. Mater.* **2008**, *18*, 1363.
[20] D. H. Lee, T. Oh, K. Cho, *J. Phys. Chem. B* **2005**, *109*, 11301.
[21] a) A. Das, S. Pisana, B. Chakraborty, S. Piscanec, S. K. Saha, U. V. Waghmare, K. S. Novoselov, H. R. Krishnamurthy, A. K. Geim, A. C. Ferrari, A. K. Sood, *Nat. Nanotechnol.* **2008**, *3*, 210; b) C. Casiraghi, *Phys. Rev. B* **2009**, *80*, 233407.
[22] a) T. O. Wehling, A. I. Lichtenstein, M. I. Katsnelson, *Appl. Phys. Lett.* **2008**, *93*, 202110; b) S. Ryu, L. Liu, S. Berciaud, Y. J. Yu, H. T. Liu, P. Kim, G. W. Flynn, L. E. Brus, *Nano Lett.* **2010**, *10*, 4944; c) K. Kim, H. J. Park, B.-C. Woo, K. J. Kim, G. T. Kim, W. S. Yun, *Nano Lett.* **2008**, *8*, 3092.
[23] a) X. R. Wang, X. L. Li, L. Zhang, Y. Yoon, P. K. Weber, H. L. Wang, J. Guo, H. J. Dai, *Science* **2009**, *324*, 768; b) X. Dong, Y. Shi, W. Huang, P. Chen, L.-J. Li, *Adv. Mater.* **2010**, *22*, 1649.
[24] D. S. Novikov, *Appl. Phys. Lett.* **2007**, *91*, 102102.
[25] Y. W. Tan, Y. Zhang, K. Bolotin, Y. Zhao, S. Adam, E. H. Hwang, S. Das Sarma, H. L. Stormer, P. Kim, *Phys. Rev. Lett.* **2007**, *99*, 246803.
[26] S. Pisana, M. Lazzeri, C. Casiraghi, K. S. Novoselov, A. K. Geim, A. C. Ferrari, F. Mauri, *Nat. Mater.* **2007**, *6*, 198.
[27] S. Bae, H. Kim, Y. Lee, X. F. Xu, J. S. Park, Y. Zheng, J. Balakrishnan, T. Lei, H. R. Kim, Y. I. Song, Y. J. Kim, K. S. Kim, B. Ozyilmaz, J. H. Ahn, B. H. Hong, S. Iijima, *Nat. Nanotechnol.* **2010**, *5*, 574.
[28] Y. Jang, D. H. Kim, Y. D. Park, J. H. Cho, M. Hwang, K. Cho, *Appl. Phys. Lett.* **2006**, *88*, 072102.